

Fluorine-incorporation scheme in fluorinated amorphous silicon prepared by various methods.

メタデータ	言語: eng 出版者: 公開日: 2017-10-03 キーワード (Ja): キーワード (En): 作成者: メールアドレス: 所属:
URL	http://hdl.handle.net/2297/24481

Fluorine-incorporation scheme in fluorinated amorphous silicon prepared by various methods

Minoru Kumeda, Yukio Takahashi, and Tatsuo Shimizu

Department of Electronics, Faculty of Technology, Kanazawa University, Kanazawa 920, Japan

(Received 16 January 1987)

Fluorinated amorphous silicon (*a*-Si:F) films are prepared by three different methods: glow-discharge decomposition of SiF₂ gas, magnetron sputtering, and conventional diode sputtering. The incorporation scheme of F atoms is investigated by means of nuclear magnetic resonance (NMR) and infrared (ir) absorption measurements. ¹⁹F NMR signals observed at 4.2 K can be simulated by superposing signals from dispersed F atoms, clustered F atoms, SiF₄ molecules, and SiF₃ species. The content of SiF₄ increases by annealing in agreement with an increase in the intensity of ir absorption at 1020 cm⁻¹. ¹⁹F NMR signals at 77 K and at room temperature show the effect of motional narrowing because SiF₄ molecules move easily in the amorphous network.

I. INTRODUCTION

Hydrogenated amorphous silicon (*a*-Si:H) is now widely applied in photovoltaic devices. The role of hydrogen in reducing defects in *a*-Si:H has been made fairly clear. Not only do hydrogen atoms play a role in terminating dangling bonds, but also dispersed H atoms relax the overcoordinated strained network structure and prevent creation of dangling bonds.¹ The incorporation scheme of H atoms in *a*-Si:H has been investigated by means of nuclear magnetic resonance (NMR). It is known that the NMR signal of H atoms in *a*-Si:H can be deconvoluted into two components, a narrow Lorentzian line and a broad Gaussian line, which are attributed to dispersed H atoms and clustered H atoms, respectively.²

Fluorinated amorphous silicon (*a*-Si:F) is more heat resistant than *a*-Si:H.³ However, *a*-Si:F with defect densities as low as that in device-quality *a*-Si:H has not yet been fabricated. It is generally considered that F atoms act as dangling-bond terminators like H atoms, but the role of F atoms in reducing dangling bonds is not clear so far. From an analogy with the role of dispersed H atoms which are effective in reducing dangling bonds,¹ it is expected that F atoms in the form of dispersed monofluoride (SiF) might play a role in reducing dangling bonds.

According to Janai and co-workers,⁴ H atoms in *a*-Si:H are incorporated in pairs by selectively dissociating strained Si—Si bonds because the Si—H bond strength is slightly lower and almost equal to the Si—Si bond strength, while F atoms in *a*-Si:F are incorporated randomly in the Si network because the Si—F bond strength is much higher than the Si—Si bond strength. They also suggested that these randomly incorporated F atoms will contribute to the narrow NMR line as do the dispersed H atoms in *a*-Si:H, whereas the broad NMR line should be attributed to SiF₄ molecules.

Recent NMR,^{5,6} infrared (ir) absorption,⁷ and calorimetric^{8,9} studies have revealed concrete evidence of the existence of H₂ molecules in *a*-Si:H. We have reported evidence of the existence of SiF₄ molecules in *a*-Si:F films by means of NMR.¹⁰

In the present work, *a*-Si:F films prepared by various

methods are investigated by means of ir and NMR measurements. Changes by annealing are also investigated in order to see the changes in the incorporation scheme of F atoms. One of the purposes of the present work is to test the suggestion made by Janai *et al.*⁴

II. EXPERIMENTAL

a-Si:F films were prepared by three different methods: (1) glow-discharge (GD) decomposition of SiF₂ gas, (2) magnetron sputtering (MS), and (3) conventional diode sputtering (DS). In all three methods, rf power (13.56 MHz) was supplied to the discharge chamber. Sample films were deposited on aluminum-foil substrates, crystalline-silicon substrates, and glass substrates. In the GD method, SiF₄ gas was introduced in a furnace in which debris of crystalline silicon was kept at 1120°C to create SiF₂ gas.^{11,12} The SiF₂ gas mixed with the undecomposed SiF₄ gas was then introduced in the discharge chamber. In the MS and DS methods, a crystalline-silicon target was sputtered in a gas mixture of Ar and SiF₄. Table I shows the deposition parameters for the different methods.

Pulsed NMR measurements were performed at 16 MHz at 4.2 K, 77 K, and room temperature for films deposited on aluminum-foil substrates. The films had been removed from the substrates by dissolving the substrates in dilute HCl solution and had then been dried in an oven at 50°C. The F content was determined by comparing the NMR signal intensity of the film with that of a standard sample (C₆H₅F). Free induction decay (FID) signals following 90° pulses were accumulated by using a digital storage oscilloscope. Since our NMR apparatus employs single-phase detection, a deviation of the resonant frequency from the resonance condition would lead to a ringing of the FID curve. In order to ascertain that the shape of the observed FID curve is not caused by the off-resonance condition, the resonant frequency was carefully determined before data acquisition by increasing and decreasing the frequency so that a small amount of frequency deviation in both directions around the resonant frequency gave the coincident signal on an oscilloscope.¹³

TABLE I. Sample preparation conditions and F content determined by NMR.

Method	Gas	Pressure or flow rate	rf power (W)	Substrate temperature (°C)	F content (at. %)
GD	SiF ₂ +SiF ₄	10 cm ³ at STP	20	300	~5
MS	Ar + SiF ₄ (10%)	0.7 Pa	200	300	~11-15
DS	Ar + SiF ₄ (8%)	1.3 Pa	250	100	~18

The accumulated FID signal was then transformed into the frequency domain by fast Fourier transform. The spectrum in the frequency domain was fit by a spectrum simulated by superposing several spectra of different origins. Our measurement system had a dead time of ~ 10 μsec at 4.2 K. Since the FID signal changes largely within the first 50 μsec as shown in Fig. 1, the loss of the data within the dead time of 10 μsec might have a serious effect on the overall signal shape. Hence the effect of dead time on the Fourier-transformed signal shape was checked by using a FID curve whose Fourier-transformed signal had a Gaussian shape with full width at half maximum (FWHM) of 20 kHz. Although the deviation between the theoretical Gaussian curve and the curve obtained by Fourier-transforming the FID with a dead time is fairly large when the dead time is taken to be 20 μsec , it is almost negligible for the use of the fitting procedure when the dead time is taken to be 10 μsec . Although the observed spectrum in the frequency domain which is obtained by Fourier-transforming the observed FID does not have a Gaussian shape but has some weak structure, we assume that the effect of the dead time is also negligible. After fitting the observed spectrum in the frequency domain by superposing several spectra with different intensities and linewidths, each of which originates from specific types of F-incorporation scheme, the simulated spectrum is inversely Fourier-transformed into the time domain and the simulated FID is compared with the observed FID. At this stage the fit was almost satisfactory, but if there was a deviation between the simulated FID and the observed FID, the fitting procedure in the frequency domain was repeated.

Fourier-transformed ir measurements were made at room temperature on films deposited on crystalline-silicon substrates. The sample was set so that the angle between the normal direction to the film surface and the incident beam direction was Brewster's angle ($\sim 73^\circ$). Then the angle was slightly increased and decreased until the fringe pattern due to the interference within the film thickness disappeared.

III. RESULTS

Figure 1 shows free induction decay (FID) curves of NMR for F atoms in as-deposited and annealed *a*-Si:F films observed at 4.2 K for (a) MS and (b) GD films. Unlike the FID curves for H atoms in *a*-Si:H those for F atoms in *a*-Si:F exhibit a hollow at around 50 μsec . Moreover, this hollow is deepened by annealing as seen from the figure. Similar hollows in FID curves are also observed for F atoms in the as-deposited DS film.¹⁰

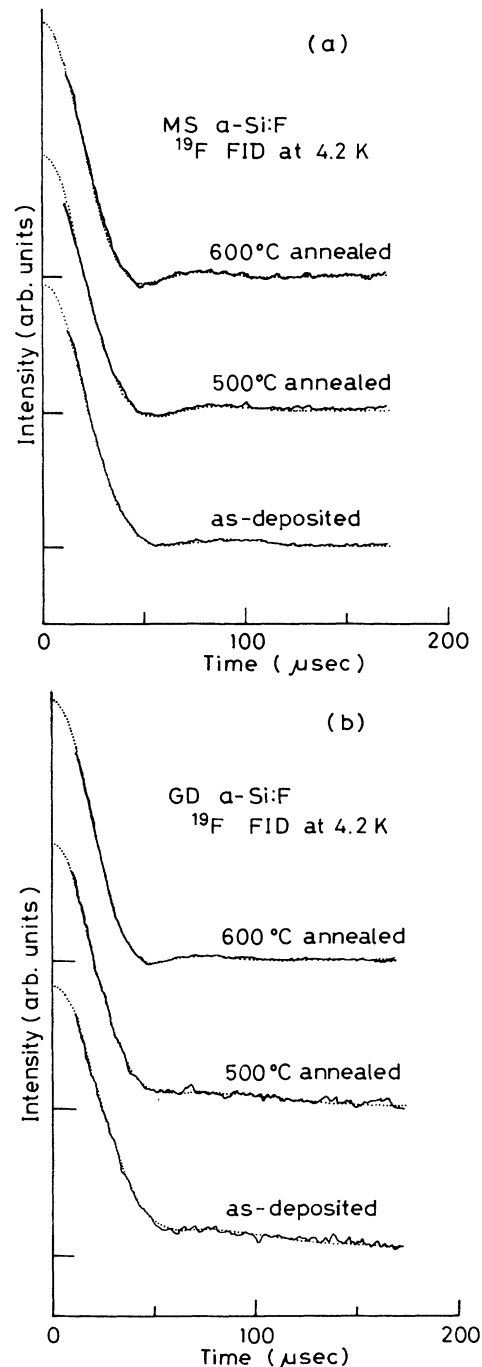


FIG. 1. FID curves of ¹⁹F NMR at 4.2 K for as-deposited and annealed *a*-Si:F films: (a) MS *a*-Si:F and (b) GD *a*-Si:F. The dotted curves are drawn by simulation (see text).

Hence these characteristic hollows indicate that the incorporation of F atoms in *a*-Si:F films is different from that of H atoms in *a*-Si:H films.

Figure 2 shows FID curves observed at 77 K for (a) MS and (b) GD films. It should be noted that for the MS film annealed at 600°C there appears an elongated tail which corresponds to an absorption signal with a narrow linewidth in the frequency domain. This narrow line is determined to be caused by motional narrowing because it does not appear at 4.2 K. A similar motional

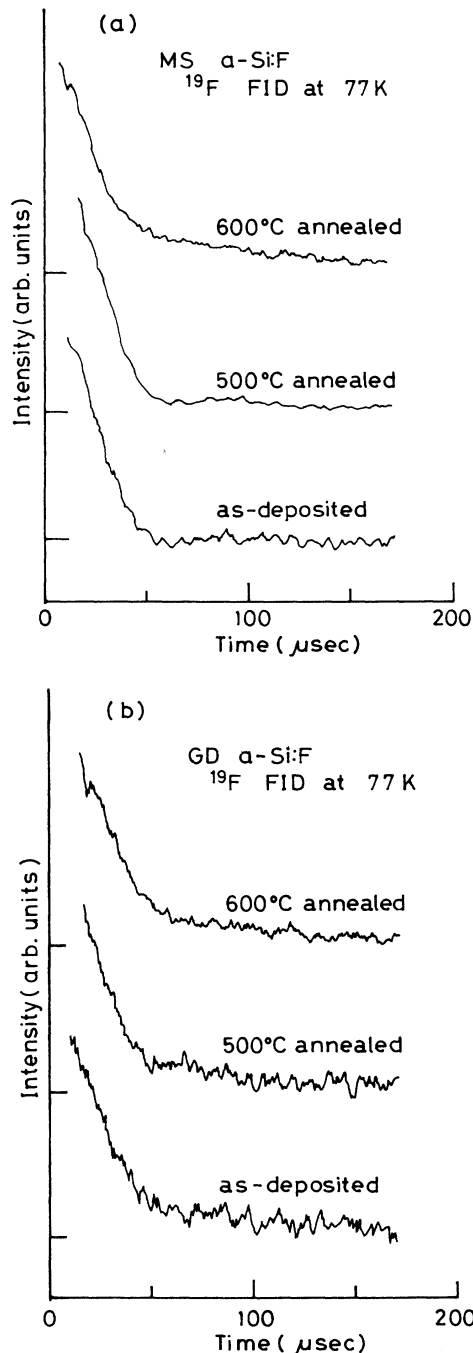


FIG. 2. FID curves of ^{19}F NMR at 77 K for as-deposited and annealed *a*-Si:F films: (a) MS *a*-Si:F and (b) GD *a*-Si:F.

narrowing is also clearly seen at 77 K for the GD film annealed at 600°C by comparing the FID curves at 77 K [Fig. 2(b)] and at 4.2 K [Fig. 1(b)]. Although the GD film was not large enough to be measured at room temperature, motional narrowing was found to become prominent for the as-deposited and the annealed MS films and the as-deposited DS film as the temperature was increased to room temperature. The NMR signals for the MS films at room temperature can be fitted by a single Lorentzian line whose linewidth decreases upon annealing. The NMR signal for the DS film at room temperature also has a dominant contribution from the narrow Lorentzian line, but a Gaussian component of about one-third of the total F atoms is also included. These results on motional narrowing indicate that in all the *a*-Si:F films there exist F atoms which can easily move.

Figure 3 shows the temperature dependence of the spin-lattice relaxation time T_1 . Although the number of temperatures at which measurements were done is limited, it is found that the films annealed at 600°C exhibit a minimum at a lower temperature than the as-deposited films.

Figure 4 shows the change of the ir spectrum upon annealing for (a) MS and (b) GD films. The intensity of the peak at 1020 cm^{-1} increases and that at 830 cm^{-1} decreases upon annealing. The result is qualitatively similar to those already reported.¹⁴⁻¹⁶ In the GD films, there appears an ir peak at 750 cm^{-1} which is considered to originate from the Si-F-Si configuration.^{17,18}

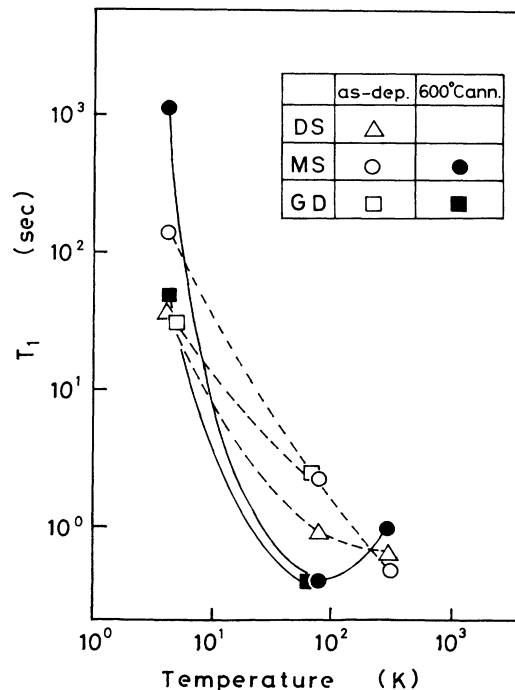


FIG. 3. Temperature dependence of the spin-lattice relaxation time T_1 .

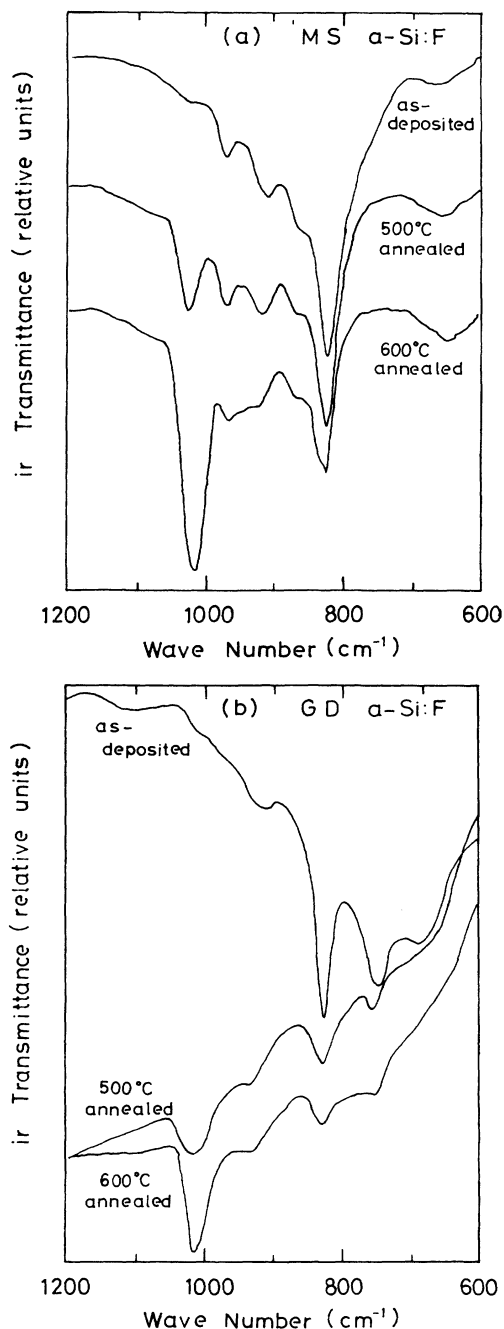


FIG. 4. ir spectra for as-deposited and annealed *a*-Si:F films: (a) MS *a*-Si:F and (b) GD *a*-Si:F.

IV. DISCUSSION

An important feature of the FID curves for ^{19}F NMR in *a*-Si:F films is a hollow at around $50 \mu\text{sec}$, which increases upon annealing, as shown in Fig. 1. We assume that the NMR signals at 4.2 K are no more affected by motional narrowing, although those observed at 77 K and at room temperature are affected by it. Then, by analyzing those FID curves at 4.2 K having a hollow, we can obtain a knowledge of the F-atom incorporation scheme. We first try to analyze the most prominent case

of 600°C -annealed MS *a*-Si:F in Fig. 1. The FID curve is converted into an NMR signal in the frequency domain by Fourier transformation. The NMR signal exhibits a weak shoulder (see Fig. 6), which can not be deconvoluted into a broad Gaussian line and a narrow Lorentzian line unlike the ^1H NMR signals in *a*-Si:H, but requires a double-peaked line in addition to a Gaussian line or a Lorentzian line to reproduce the observed signal.

Since F atoms have a larger chemical shift than H atoms, the double-peaked line might be attributed to two ^{19}F resonance lines with different chemical shifts arising from different bonding schemes. The difference in the chemical shifts of SiF, SiF₂, SiF₃, and SiF₄ is estimated to be of the order of 10^{-4} judging from the difference in chemical shifts for $\text{Me}_x\text{SiF}_{4-x}$ and $\text{Et}_x\text{SiF}_{4-x}$ compounds ($x=0,1,2,3$), where Me and Et denote a methyl group and an ethyl group, respectively.¹⁹ The chemical shift of 10^{-4} produces a frequency shift of 1.6 kHz. Therefore, it is improbable that the separation between the peaks of the double-peaked line of about 20 kHz [see Fig. 6(a)] arises from chemical shifts.

It is known that interacting multiple spins (two, three, four, etc.), which are identical with each other and are only weakly coupled with other spins, exhibit a powder-pattern signal with multiple peaks when their molecular axes are oriented randomly with respect to the static magnetic field.²⁰ Thus the observed weak shoulder can be attributed to weakly coupled SiF₂, SiF₃, or SiF₄ groups. Figure 5 shows NMR spectra expected to arise from these groups in the frequency domain. ^{19}F NMR

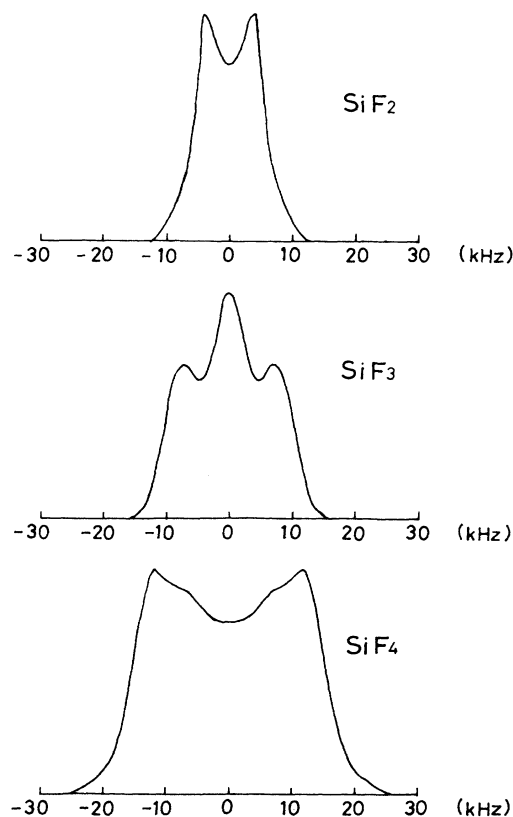


FIG. 5. ^{19}F NMR spectra expected for SiF₂, SiF₃, and SiF₄.

line shapes for SiF_2 bonded to two Si atoms and SiF_3 bonded to one Si atom were obtained from ^1H NMR line shapes observed for $\text{CaSO}_4 \cdot 2\text{H}_2\text{O}$ and $\text{CCl}_3\text{-CH}_3$ (Refs. 20 and 21) by scaling the frequency axis by considering the difference between H-H separation (1.58 Å for H_2O and 1.79 Å for CH_3) and F-F separation (2.55 Å) and also the difference in the magnetogyric ratios for ^1H ($\gamma_{\text{H}} = 2.675 \times 10^4 \text{ s}^{-1} \text{ G}^{-1}$) and ^{19}F ($\gamma_{\text{F}} = 2.517 \times 10^4 \text{ s}^{-1} \text{ G}^{-1}$). Here we assumed C—H and Si—F bond lengths to be 1.09 and 1.56 Å, respectively, and the angles between the C—H and Si—F bonds to be 109.5° . The ^{19}F NMR line shape for SiF_4 molecules was obtained by changing the frequency scale of the signal arising from CF_4 (Ref. 22) by taking account of the ratio of the length of a Si—F bond to that of a C—F bond (1.34 Å). As seen from Fig. 5, the separation between shoulders expected from SiF_2 and SiF_3 seems to be too small to explain the observed shoulders (see Fig. 6). Hence we try to reproduce the observed signal by assuming the presence of SiF_4 molecules.

By superposing a spectrum arising from SiF_4 on a broad Gaussian spectrum, we can simulate the observed spectrum for 600°C -annealed MS α -Si:F. Similar simulation procedures were tried for other films, but we could

not obtain such a good agreement between the simulated signals and the observed ones within the restriction of superposing only a spectrum arising from SiF_4 on a broad line and a narrow line.²³ We then tried to add a contribution from SiF_3 bonded to one Si atom for signals of films other than 600°C -annealed MS α -Si:F. Best fits were obtained by the addition of SiF_3 when the F-Si-F angles were decreased slightly ($2^\circ\text{--}7^\circ$) from 109.5° . Figure 6 shows the observed signals and their deconvolution in the frequency domain.

Table II shows the results of the fitting for various films. The narrow component and the broad component are considered to arise from dispersed F atoms and clustered F atoms, respectively, just as dispersed and clustered H atoms contribute to the narrow and broad NMR lines in α -Si:H.² Dotted curves in Fig. 1 are drawn by using the parameters shown in Table II. As seen from the table, the fraction of SiF_4 molecules increases with increasing annealing temperature for both MS and GD films. The results shown in Table II are different from the suggestion of Janai *et al.*, that the F atoms in α -Si:F are only in the form of SiF_4 and dispersed SiF species.⁴

In Fig. 7 we compare the fraction of F atoms in the form of SiF_4 with the fraction of the intensity of the ir ab-

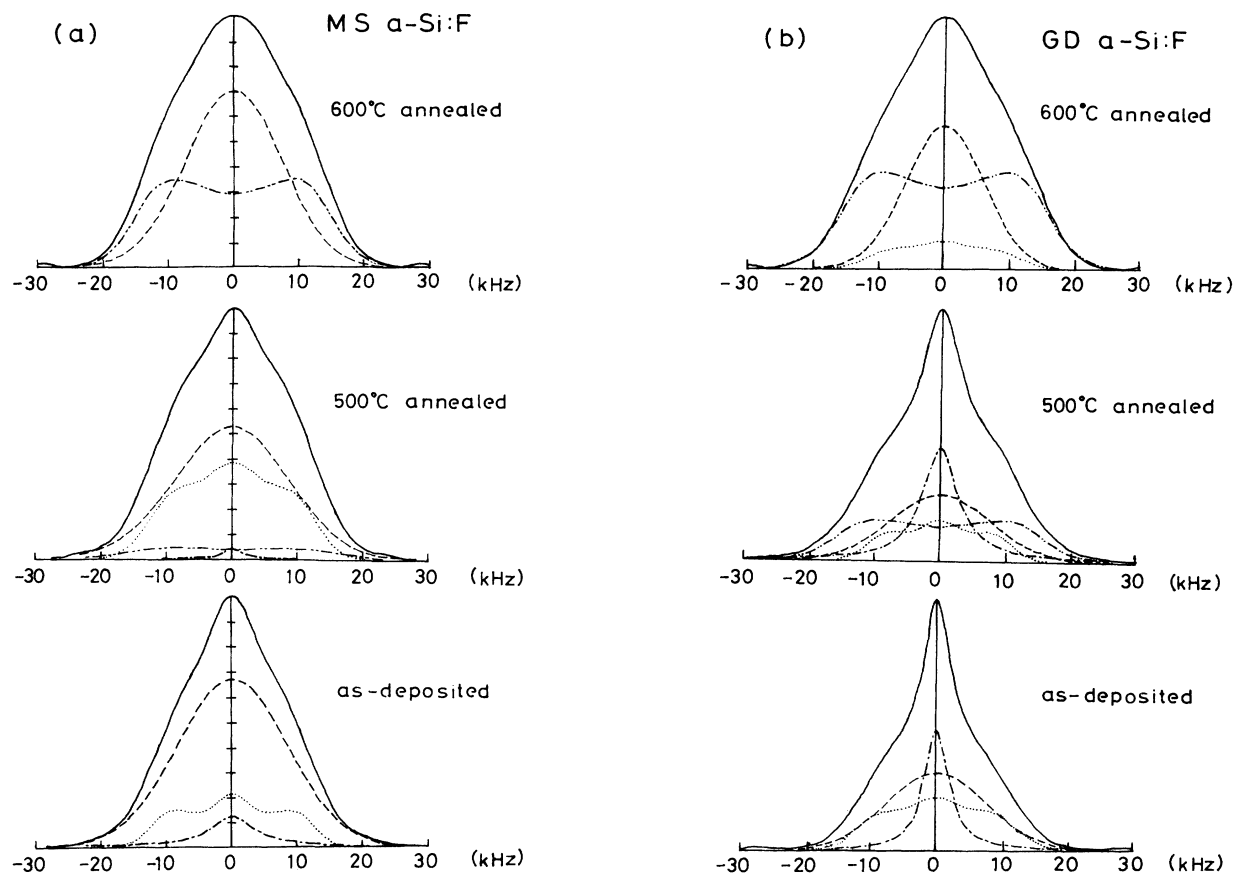


FIG. 6. ^{19}F NMR signals observed at 4.2 K (solid curves) are deconvoluted into a narrow Lorentzian line (dot-dashed curves), a broad Gaussian line (dashed curves), a line from SiF_4 molecules (dot-dot-dashed curves), and a line from SiF_3 species (dotted curves): (a) MS α -Si:F and (b) GD α -Si:F. The sum of the component lines is not shown because it is almost hidden under the observed curve in most parts.

TABLE II. Results of deconvolution of the NMR signals observed at 4.2 K into a narrow Lorentzian line, a broad Gaussian line, a line arising from SiF₄ molecules, and a line arising from SiF₃ species. Percentages of component lines to simulate the observed signals are shown. Line widths (full width at half maximum) are also shown for the narrow component and the broad component.

Sample	Anneal	Narrow	Broad	SiF ₄	SiF ₃
MS	as-deposited	7.3% 8.4 kHz	72.3% 19.9 kHz	0%	20.4%
	500 °C	1.2% 4.1 kHz	52.9% 20.2 kHz	7.3%	38.6%
	600 °C	0%	54.8% 17.3 kHz	45.2%	0%
GD	as-deposited	23.0% 4.3 kHz	44.2% 18.0 kHz	0%	32.8%
	500 °C	24.8% 6.6 kHz	28.9% 18.0 kHz	29.7%	16.6%
	600 °C	0%	37.3% 14.1 kHz	53.2%	9.5%
DS	as-deposited	5.2% 4.2 kHz	56.4% 18.5 kHz	25.9%	12.5%

sorption at 1020 cm⁻¹ in the integrated intensity for all the ir absorptions arising from Si-F stretching vibrations for various films with and without annealing. The fact that the fraction of the 1020-cm⁻¹ absorption is close to the fraction of SiF₄ obtained by NMR measurements strongly supports the identification of this ir peak with SiF₄.¹⁴⁻¹⁶ It is not reasonable to assign the 1020-cm⁻¹ ir peak to SiF₃,^{24,25} because after annealing at 600 °C this peak increases as shown in Fig. 4, while the fraction of SiF₃ decreases as seen from Table II.

Moreover, the result in Fig. 7 indicates that the oscillator strengths for the ir absorption peaks are not different between the 1020- and 830-cm⁻¹ peaks. A constant oscillator strength for the different ir peaks is also obvious

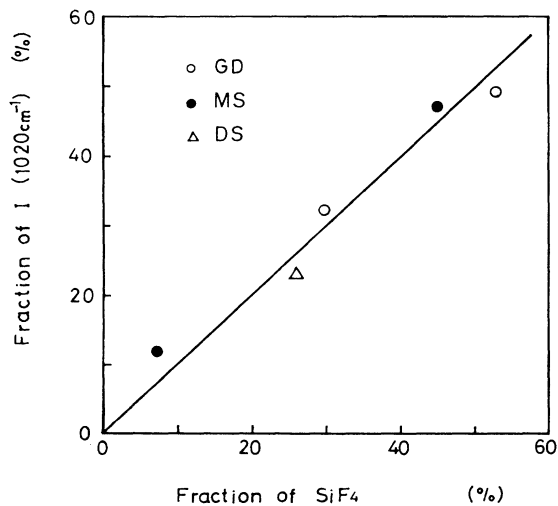


FIG. 7. The fraction of F atoms in the form of SiF₄ molecules obtained from NMR vs the fraction of the intensity of the ir absorption at 1020 cm⁻¹ in the integrated intensity for all the ir absorption arising from Si-F stretching vibrations for various films with and without annealing.

since the integrated intensity of the ir absorption in Fig. 4 is roughly constant, although annealing makes the 830-cm⁻¹ peak decrease and the 1020-cm⁻¹ peak increase. The fact that the oscillator strength for the Si-F stretching vibration is unchanged for the different absorption peaks is in contrast to the proposal by Cardona that the oscillator strength of the Si-H stretching vibration at 2100 cm⁻¹ is quite different from that at 2000 cm⁻¹ in *a*-Si:H.²⁶

We now compare the results in Table II obtained at 4.2 K with those in Fig. 2 at 77 K. Although the 600 °C-annealed films have no narrow component at 4.2 K as seen from Table II, these films exhibit slow FID decays corresponding to a narrow component at 77 K as shown in Fig. 2. The NMR signals at 77 K for 600 °C-annealed films can be deconvoluted into a broad Gaussian line and a narrow Lorentzian line. Since SiF₄ molecules are expected to move easily as temperature increases, the prominent effect of motional narrowing as shown in Fig. 2 is expected to originate from the motion of SiF₄ molecules. The correlation time for motion, τ_c , can be estimated from the narrowed linewidth by using an expression,

$$(\delta\omega)^2 = (\delta\omega_0)^2 \frac{2}{\pi} \tan^{-1}(\alpha\delta\omega\tau_c),$$

where $\delta\omega$ is the narrowed linewidth, $(\delta\omega_0)^2$ the second moment of the rigid lattice, and α a numerical factor of order unity.²⁰ If we take the full width at half maximum (FWHM) at 4.2 K for $\delta\omega_0$ and the FWHM of the narrowed line at 77 K for $\delta\omega$ and $\alpha=1$, we get $\tau_c \sim 3.6 \times 10^{-6}$ sec and $\tau_c \sim 4.0 \times 10^{-6}$ sec at 77 K for MS and GD films annealed at 600 °C, respectively. The value of τ_c for F atoms in fluorinated and hydrogenated amorphous silicon [*a*-Si:(F,H)] reported previously is close to these values at 77 K and decreases at higher temperature.²⁷ In the NMR signals at 77 K for 600 °C-annealed films, the fractions of the narrow components are 30% and 26% for MS and GD films, respectively. Comparing these percentages with 45.2% and

53.2% of the SiF₄ fractions for 600 °C–annealed MS and GD films, respectively, we conclude that a part of the SiF₄ molecules does not move rapidly enough to make the NMR line motionally narrowed at 77 K. The fact is consistent with the previous result that τ_c further decreases above 77 K.²⁷

In the temperature dependence of the spin-lattice relaxation time T_1 shown in Fig. 3, the minimum occurs at lower temperature for the 600 °C–annealed films than for the as-deposited films. It is possible that the increase in movable SiF₄ molecules by annealing brings the shift of the T_1 minimum, but a detailed mechanism of the temperature dependence of T_1 is not clear at present.

We previously reported on the relation between the density of dangling bonds and the H-incorporation scheme in *a*-Si:H films: Dispersed H atoms which contribute to the narrow component of the NMR signal have a role in reducing the density of dangling bonds.²⁸ About 5 at. % of dispersed H atoms can reduce the density of dangling bonds to $\sim 10^{16}$ cm⁻³. F atoms are expected to have the same role as H atoms in the sense that singly coordinated F atoms bond with dangling bonds and terminate them. However, the density of dispersed F atoms which contribute to the narrow component of the NMR signal is at most 1.2 at. % in our samples of MS, GD, and DS *a*-Si:F films, and the density of dangling bonds measured by electron spin resonance is 8.4×10^{18} cm⁻³ to 1.8×10^{19} cm⁻³. Hence we cannot say whether the dispersed F atoms in *a*-Si:F have the same role as the dispersed H atoms in *a*-Si:H. Sample films with a large amount of dispersed F atoms are needed to answer this question.

V. CONCLUSION

The incorporation scheme of F atoms in *a*-Si:F films prepared by (1) glow-discharge decomposition, (2) magnetron sputtering, and (3) conventional diode sputtering was investigated by means of NMR and ir measurements. The FID curves of ¹⁹F NMR at 4.2 K have a characteristic hollow at around 50 μsec which is not observed for ¹H NMR in *a*-Si:H films. The observed NMR signals can be simulated by superposing signals from dispersed F atoms, clustered F atoms, SiF₄ molecules, and SiF₃ species. By annealing at 600 °C, the content of SiF₄ molecules estimated from the simulation of the NMR signal and the intensity of the ir absorption at 1020 cm⁻¹ increase. Since these two quantities are close for all films, the ir absorption at 1020 cm⁻¹ is considered to originate from SiF₄ molecules. Since SiF₄ molecules are easy to move in the amorphous network, a prominent effect of motional narrowing is observed at 77 K and at room temperature for NMR signals for 600 °C–annealed films.

ACKNOWLEDGMENTS

The authors wish to thank K. Aono and M. Toda of Central Glass Inc. for supplying the SiF₄ gas used for preparing the GD films. The authors are also grateful to A. Morimoto for the help during sample preparation, S. Nakanishi for the simulation of the NMR signals, Y. Yonezawa and H. Komatsu for early stage contributions to this work, and S. Ueda for the use of the NMR apparatus. This work was partly supported by the Sunshine Project of the Ministry of International Trade and Industry of Japan.

¹T. Shimizu, *J. Non-Cryst. Solids* **59&60**, 117 (1983).

²J. A. Reimer, *J. Phys. (Paris) Colloq.* **42**, C4-715 (1981).

³H. Matsumura, Y. Nakagome, and S. Furukawa, *Appl. Phys. Lett.* **36**, 439 (1980).

⁴M. Janai and R. A. Street, *Phys. Rev. B* **31**, 6609 (1985).

⁵W. E. Carlos and P. C. Taylor, *Phys. Rev. B* **25**, 1435 (1982).

⁶J. B. Boyce and M. Stutzmann, *Phys. Rev. Lett.* **54**, 562 (1985).

⁷Y. J. Chabal and C. K. N. Patel, *Phys. Rev. Lett.* **53**, 210 (1984).

⁸J. E. Graebner, B. Golding, L. C. Allen, D. K. Biegelsen, and M. Stutzmann, *Phys. Rev. Lett.* **52**, 553 (1984).

⁹H. V. Lohneysen, H. J. Schink, and W. Beyer, *Phys. Rev. Lett.* **52**, 549 (1984).

¹⁰M. Kumeda, Y. Yonezawa, and T. Shimizu, *Jpn. J. Appl. Phys.* **23**, L540 (1984).

¹¹M. Janai, R. Weil, and B. Pratt, *Phys. Rev. B* **31**, 5311 (1985).

¹²H. Matsumura and H. Tachibana, *Appl. Phys. Lett.* **47**, 833 (1985).

¹³E. Fukushima and S. B. W. Roeder, *Experimental Pulse NMR—A Nuts and Bolts Approach* (Addison-Wesley, Reading, Mass., 1981), Chap. 6.

¹⁴C. J. Fang, L. Ley, H. R. Shanks, K. J. Gruntz, and M. Cardona, *Phys. Rev. B* **22**, 6140 (1980).

¹⁵M. Janai, L. Frey, R. Weil, and B. Pratt, *Solid State Commun.* **48**, 521 (1983).

¹⁶K. Yamamoto, M. Tsuji, K. Washio, H. Kasahara, and K. Abe, *J. Phys. Soc. Jpn.* **52**, 925 (1983).

¹⁷L. E. Mosley, M. A. Paesler, G. Lucovsky, and A. Waltner, *Solid State Commun.* **53**, 513 (1985).

¹⁸E. W. Ignacio, H. B. Schlegel, and J. Bicerano, *Chem. Phys. Lett.* **127**, 367 (1986).

¹⁹E. Schnell and E. G. Rochow, *J. Am. Chem. Soc.* **78**, 4178 (1956).

²⁰A. Abragam, *The Principle of Nuclear Magnetism* (Oxford, New York, 1961), Chap. 7.

²¹E. R. Andrew and R. Bersohn, *J. Chem. Phys.* **18**, 159 (1950).

²²S. K. Garg, D. W. Davidson, and J. A. Ripmeester, *J. Magn. Reson.* **36**, 325 (1979).

²³T. Shimizu, M. Kumeda, H. Komatsu, and Y. Yonezawa, *J. Non-Cryst. Solids* **77&78**, 719 (1985).

²⁴T. Shimada, Y. Katayama, and S. Horigome, *Jpn. J. Appl. Phys.* **19**, L265 (1980).

²⁵Y. Nakayama, K. Akiyama, and T. Kawamura, *Jpn. J. Appl. Phys.* **22**, L754 (1983).

²⁶M. Cardona, *Phys. Status Solidi B* **118**, 463 (1983).

²⁷S. Ueda, K. Nakazawa, M. Kumeda, and T. Shimizu, *Solid State Commun.* **42**, 261 (1982).

²⁸T. Shimizu, K. Nakazawa, M. Kumeda, and S. Ueda, *Jpn. J. Appl. Phys.* **21**, L351 (1982); *Physica* **117&118B**, 926 (1983).